

## Anomalous far-infrared absorption in random small-particle composites

G. L. Carr, R. L. Henry, N. E. Russell, J. C. Garland, and D. B. Tanner

*Department of Physics, The Ohio State University, Columbus, Ohio 43210*

(Received 23 December 1980)

The frequency dependence and magnitude of the far-infrared absorption of a small-metal-particle composite material has been measured over the range of 4–100  $\text{cm}^{-1}$ . The composite samples consisted of spherical metal particles, with radii varying from 100–1000 Å, randomly dispersed in an insulating host. In some samples, a nonlinear dependence of the absorption on the metal-particle concentration was observed, indicating that interparticle interactions can play an important role. It is shown that the magnitude of the absorption cannot be explained by classical electromagnetic theory.

### I. INTRODUCTION

An intriguing result found in previous investigations<sup>1-4</sup> of small-particle-composite systems is that the far-infrared absorption is considerably larger than predicted by classical electromagnetic theory. Although the classical theory gives the correct frequency dependence, it falls short of predicting the correct magnitude by 1 to 3 orders of magnitude. This failure is particularly surprising in view of the successes of the classical theory (Mie theory) in accounting for both the absorption and the scattering of visible light by small particles.

One suggestion, made originally by Simanek<sup>5</sup> and elaborated by Ruppin,<sup>6</sup> attributes the large far-infrared absorption to the oxide coating on the surface of the particles. Simanek was able to calculate a far-infrared absorption which was within a factor of 2 of the data on very small Al particles studied by Granqvist *et al.*,<sup>2</sup> while Ruppin obtained an absorption that exceeded the experimental data of Tanner *et al.*<sup>1</sup> on somewhat larger Al particles.

The far-infrared absorption of  $\sim 1\text{-}\mu\text{m}$  radius Pd particles was discussed recently by Russell *et al.*<sup>4</sup> and was found to exceed theoretical predictions by about a factor of 10. In this paper we present the results of a study of the absorption in composite systems containing much smaller ( $\sim 100\text{--}1000$  Å radii) particles. These particles, of Al, Ag, Au, or Pd, were prepared by a gas-evaporation technique and were in most cases randomly dispersed in an insulating KCl host. For most samples the absorption coefficient was found to be a linear function of the metal volume fraction. Our Al composite samples, however, differed significantly from those containing other metals; for Al the concentration dependence was nearly quadratic. In all cases, the magnitude of the absorption was larger than predicted by the classical theory. Our results indicate that

the anomalous absorption cannot be attributed to oxide coatings on the particle surfaces.

### II. REVIEW OF CLASSICAL ELECTROMAGNETIC THEORY

The optical properties of an inhomogeneous medium are described by a complex dielectric function and a complex magnetic permeability, each a function of position. In a two-component metal-insulator mixture, the dielectric function has two possible values,

$$\epsilon = \epsilon(\vec{r}) = \begin{cases} 1 - \frac{\omega_p^2}{\omega^2 + i\omega/\tau} = \epsilon_m & (\vec{r} \text{ in metal}) \\ \epsilon_i & (\vec{r} \text{ in insulator}), \end{cases} \quad (1)$$

where we have taken a Drude dielectric function for the metal, with  $\omega_p$  the plasma frequency and  $\tau$  the scattering time for electrons. The insulator is assumed to have a dielectric constant which is a frequency-independent real number.

The characterization of the inhomogeneous material by  $\epsilon(\vec{r})$  is obviously not very useful because one needs to know the exact geometrical arrangement of the constituents of the material. However, if the wavelength of the electromagnetic radiation is much larger than the particle size, the classical theories<sup>7-12</sup> of inhomogeneous media presume that the material can be treated as a homogeneous substance with an effective dielectric function and effective magnetic permeability. These quantities depend upon the properties of the constituents, as well as their volume fractions and sizes, i.e.,

$$\epsilon = \epsilon(\epsilon_m, \epsilon_i, f, a). \quad (2)$$

In Eq. (2),  $f$  is the volume fraction of the metallic constituent ( $1 - f$  will then be the volume fraction of the insulator) and  $a$  is the median particle size. Theories for the effective far-infrared properties of a composite medium have been discussed recently by Russell *et al.*<sup>4</sup> The results will be

summarized here.

There are two effective-medium theories commonly used to describe inhomogeneous media. The first, known as the Maxwell Garnett theory (MGT), is an unsymmetrical molecular field model<sup>8</sup> that gives for the dielectric function

$$\epsilon_g = \epsilon_i + \frac{3f\epsilon_i(\epsilon_m - \epsilon_i)}{(1-f)\epsilon_m + (2+f)\epsilon_i} \quad (3)$$

This function is found by averaging the electric fields and polarizations (induced by the applied electric field) in the composite medium.

The second theory is a symmetric self-consistent model known as the effective-medium approximation (EMA).<sup>9</sup> (Actually, both theories are effective-medium theories.) The EMA yields a quadratic equation for the dielectric function. The principal difference between the two theories is that only the EMA predicts a metal-insulator transition in the composite at a critical metal volume fraction,  $f_c$ . For  $f < f_c$  the material is an insulator while for  $f > f_c$  it is a conductor. Although the EMA predicts  $f_c = \frac{1}{3}$  for spherical particles in three-dimensional samples, random composites have  $0.17 \leq f_c \leq 0.22$ . Both theories predict an optical resonance at high frequencies, near  $\omega_g = \omega_p [(1-f)/3\epsilon_i]^{1/2}$ , with the MGT predicting a sharper resonance. The far-infrared electric dipole absorption results from the low-frequency tail of this resonance.

For our purposes, it is important to note that the MGT and the EMA give almost identical results for the far-infrared properties at low concentrations ( $f < 0.05$ ) of metal in insulator. Because of this similarity we will use the simple MGT rather than the physically more appealing EMA.

In addition to the electric dipole absorption described above, a metal particle composite has a second mechanism for absorption arising from the effects of the magnetic field of the incident radiation. This magnetic field will induce eddy currents in the conducting particles which give the material an inhomogeneous magnetization.<sup>1,4,10,11</sup> The effective permeability of the composite will thus not be unity because of this magnetization—even though the permeability of the constituents may be exactly unity.

The magnetic polarizability of the particles is given by<sup>13</sup>

$$\gamma_m = \frac{3}{8\pi} \frac{j_2(ka)}{j_0(ka)} = \frac{3}{8\pi} \left( \frac{3}{(ka)^2} - 1 - \frac{3}{(ka)} \cot(ka) \right), \quad (4)$$

where  $j_0$  and  $j_2$  are spherical Bessel functions and  $k = \omega\epsilon^{1/2}/c$  is the propagation constant for electromagnetic waves in the metal.

Using Eq. (4), the effective permeability of the

composite resulting from the induced magnetic dipoles may be calculated using the MGT or EMA in a way completely analogous to that used to calculate the effective dielectric function. The MGT permeability, which we will use, is identical in form to Eq. (3)

$$\mu_g = 1 + \frac{3f(\mu_m - 1)}{(1-f)\mu_m - (2+f)}, \quad (5)$$

where we have set the permeability of the insulator equal to unity. The permeability of the metal is related to the magnetic polarizability in the usual way, i.e.,

$$\mu_m = \frac{1 + (8\pi/3)\gamma_m}{1 - (4\pi/3)\gamma_m} \quad (6)$$

The absorption coefficient of the inhomogeneous medium is given by

$$\alpha = \frac{2\omega}{c} \text{Im}(\epsilon_g \mu_g)^{1/2} \quad (7)$$

At low frequencies and small volume fractions, Eqs. (3)–(7) may be combined to give the following expression for the absorption coefficient:

$$\alpha = \frac{f\omega^2}{c^2} \left( \frac{9c}{\omega_p^2 \tau} + \frac{a^2 \omega_p^2 \tau}{10c} \right) \quad (8)$$

In Eq. (8) the first term represents the electric dipole absorption and the second the magnetic dipole absorption. The magnetic dipole term dominates the electric dipole term for  $a > 30 \text{ \AA}$ . The criteria for making the approximations that give Eq. (8) are

$$\omega \ll 1/\tau,$$

$$a \ll \delta,$$

$$f \ll f_c,$$

where  $\delta$  is the classical skin depth. These criteria are satisfied for far-infrared frequencies, particle radii smaller than  $100 \text{ \AA}$ , and volume fractions below a few percent.

Equation (8) may be written in a convenient form by setting

$$\alpha = K f \omega^2, \quad (9)$$

where  $K$  depends upon the particle radius  $a$  and dc conductivity  $\sigma_0 = \omega_p^2 \tau / 4\pi$ . For typical values  $a \approx 500 \text{ \AA}$  and  $\sigma_0 \approx 10^6 \Omega^{-1} \text{ cm}^{-1}$  (the conductivity most metals would have if the mean free path were equal to the radius  $a$ ) then  $K \approx 0.02 \text{ cm}$ . (With  $\omega$  in  $\text{cm}^{-1}$ ,  $K$  is in  $\text{cm}$  to give  $\alpha$  in  $\text{cm}^{-1}$ .) This absorption is almost entirely magnetic dipole. If only electric dipole absorption occurs, then  $K \approx 10^{-5} \text{ cm}$ .

Figure 1 shows the electric dipole absorption coefficients calculated for Al particles in KCl

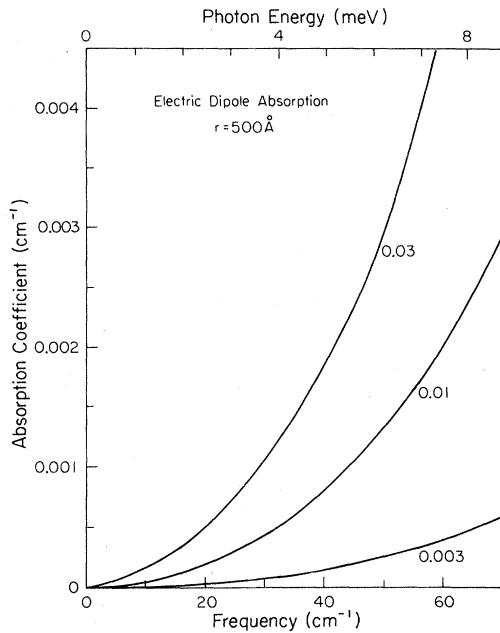


FIG. 1. Far-infrared absorption coefficient of 500-Å Al particles calculated assuming only electric dipole absorption. The absorption coefficient is shown for metal volume fractions of 0.003, 0.01, and 0.03.

host using Eqs. (1), (3), and (7) with  $\mu_g = 1$ . The mean free path of the electrons was assumed to be equal to particle radius of 500 Å. Note that the quadratic frequency dependence persists over the entire frequency range, as does the linear

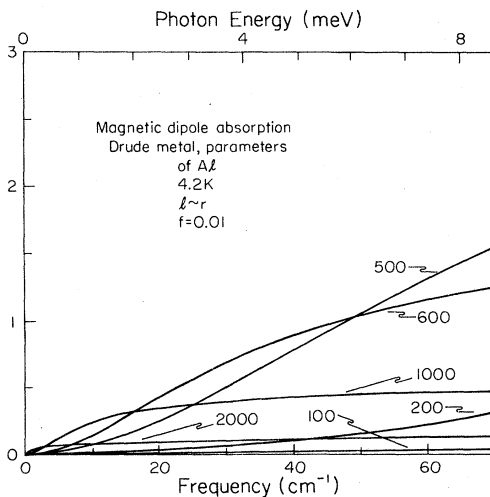


FIG. 2. Far-infrared absorption coefficient of Al particles calculated assuming only magnetic dipole absorption. The metal volume fraction is 0.01. The absorption coefficient has been calculated for particle radii of 100, 200, 500, 600, 1000, and 2000 Å, assuming that the electronic mean free path equals the particle radius.

concentration dependence.

Figure 2 shows the magnetic dipole absorption, calculated exactly from Eqs. (4)–(7) rather than from the approximation Eq. (8). Curves are shown for several particle radii ranging between 100–1000 Å. As may be seen from the figure, the absorption coefficient is quadratic at low frequencies but tends to level off at higher frequencies. The onset of this saturation occurs at lower and lower frequencies as the particle radius increases. The saturation is a result of the skin effect, which causes the fields to be screened from the interior of the particle, reducing the amount of volume in which absorption can take place.<sup>4</sup>

### III. EXPERIMENTAL DETAILS

The small metal particles used in this study were prepared by evaporation of Au, Ag, Al, or Pd in the presence of a few Torr pressure of an inert-gas-oxygen mixture. This technique, which has been described in detail by Granqvist and Buhrman,<sup>14</sup> produces a small-metal-particle “smoke.” Three factors determine the size of these particles: the type of gas, the pressure of the gas, and the evaporation rate. Larger particles are obtained by increasing either the molecule weight of the gas, the pressure, or the temperature of the evaporation source.

A prepared mixture of argon and oxygen was passed through the bell jar during the evaporation. The oxygen caused an oxide coating to form on the particles which prevented them from cold-welding together during the evaporation process. If the oxygen were not present, the smoke was found to be electrically conducting and quite opaque. The flow rate of the gas mixture was sufficient to ensure several changes of atmosphere during the evaporation. We have varied the particle size by adjusting the gas pressure, the range employed being 0.5–10 Torr. The sizes and size distributions of the small particles were subsequently measured with a scanning electron microscope.

Most of our samples consisted of small particles randomly imbedded in a KCl host. These samples were prepared by the “KBr pellet” technique long known to infrared spectroscopists. Small particles and finely ground KCl were weighed out and thoroughly mixed. The mixture was then poured into an evacuable die and compressed into a solid pellet. The air pressure in the die at the time of compression was below 100 mTorr. The pellet was subsequently reground and recompressed from three to ten times to ensure a uniform mixture. In addition to the compacted composite, we also studied samples consisting of a mixture of

metal particles with fine powder of  $\text{Al}_2\text{O}_3$  (obtained from Linde Corporation).<sup>15</sup>

Far-infrared transmission measurements were made at 4.2 K; at this temperature the KCl was transparent to radiation below about  $70\text{ cm}^{-1}$ . Lamellar grating<sup>16</sup> and Michelson<sup>17</sup> interferometers were used as signal sources over  $4\text{--}40\text{ cm}^{-1}$  and  $20\text{--}100\text{ cm}^{-1}$ , respectively. The detector was a germanium bolometer operating at 1.2 K.

#### IV. EXPERIMENTAL RESULTS

The experimental absorption coefficient is related to the transmission coefficient  $T$ , by

$$\alpha = (1/d) \ln T - \alpha_0, \quad (10)$$

where  $d$  is the sample thickness, and  $\alpha_0$  allows for reflection losses at the front and rear sample surfaces and for detector nonlinearities. The value of  $\alpha$  is chosen so that the absorption coefficient extrapolates to zero at zero frequency.

High-resolution measurements of the absorption coefficient of the small-particle composites show an interference pattern which results from multiple internal reflections. This pattern is illustrated in Fig. 3, where the absorption coefficient is plotted versus frequency. These oscillations, only appearing at low frequencies where the absorption is small, have a spacing

$$\Delta\omega = 2\pi c/\epsilon_1^{1/2} d, \quad (11)$$

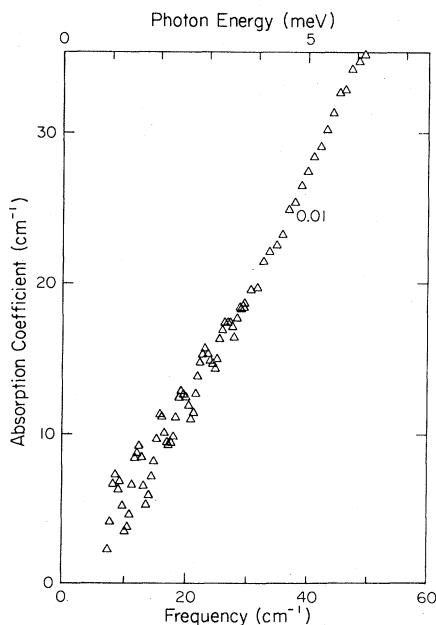


FIG. 3. Far-infrared absorption coefficient for Ag small particles in KCl. This curve illustrates the interference pattern observed when the measurements are made with high resolution.

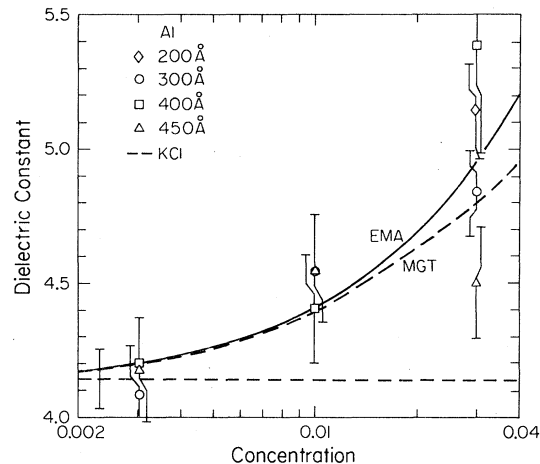


FIG. 4. Far-infrared dielectric constant of composite samples of Al in KCl, inferred from the period of the interference pattern, versus metal volume fraction.

where  $\epsilon_1$  is the dielectric constant. The dielectric constant for a number of samples inferred from the interference pattern is plotted versus concentration in Fig. 4. As expected, the dielectric constant increases with increasing concentration. The two theoretical curves shown are calculated using the MGT [Eq. (3)] and the EMA.<sup>9</sup> The scatter in the data is clearly too large to allow a choice between the two theories.

Although the presence of the interference pattern becomes a nuisance in measuring absorption coefficients, it can be eliminated by making low-resolution measurements, i.e., by reducing the number of interferogram points. The remainder of the data that we will show are from low-resolution measurements.

The far-infrared absorption coefficient of  $400\text{ \AA}$  radii Ag particles at two concentrations in KCl is shown in Fig. 5, together with absorption coefficient of pure KCl. Figure 6 shows similar data for Pd and Au small particles ( $400$  and  $700\text{ \AA}$  radii, respectively) suspended in  $\text{Al}_2\text{O}_3$  powders. The absorption coefficients of the  $\text{Al}_2\text{O}_3$  and of the polyethylene sample holder have been subtracted from the raw data to obtain the absorption coefficients shown here. The solid lines are fits of the data to Eq. (9) for the values of the coefficient  $K$  shown. Table I summarizes the results on these particles. The values for  $K$  for these samples range between 1.1 and 2.4. All of these values are more than an order of magnitude larger than the theoretical estimates calculated from Eq. (10), shown in the right-most column of the table.  $K$ , in units of cm, can be written as

$$K = 1490a^2\sigma_0, \quad (12)$$

with  $a$  in cm and  $\sigma_0 = \omega_p^2\tau/4\pi$ , the electrical con-

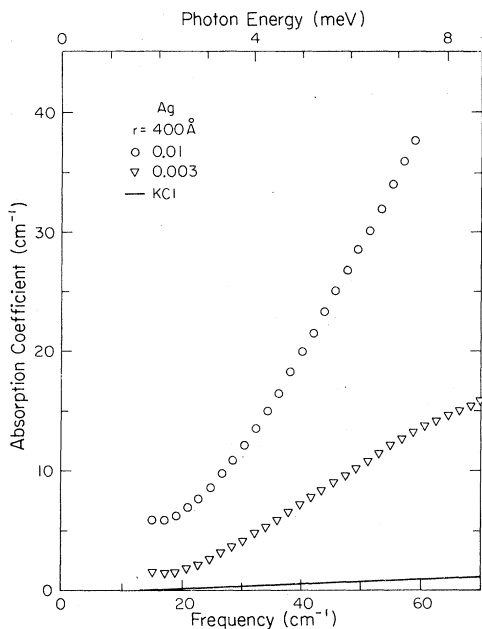


FIG. 5. Far-infrared absorption coefficient of 400-Å Ag particles in KCl. Data are shown for metal volume fractions of 0.003 and 0.01.

ductivity of the particle, in  $\Omega^{-1}\text{cm}^{-1}$ . The conductivity of the particles cannot be significantly larger than the room-temperature value because of boundary scattering.

The far-infrared absorption coefficients of composites of Al in KCl are given in Figs. 7-10, for particle radii of 150, 300, 400, and 450 Å, respectively. The volume fraction of metal in the KCl ranged from 0.003 to 0.03. The absorption coefficient of the compressed KCl is also shown in the figures. For these data, the most highly absorbing particles have 300 Å radii, while the least absorbing ones have 450 Å radii. The frequency dependence of the absorption coefficient is nearly quadratic, as shown in Fig. 11, where the data for three  $f = 0.01$  samples is plotted logarithmically.

In contrast to the absorption of Au, Pd, and Ag

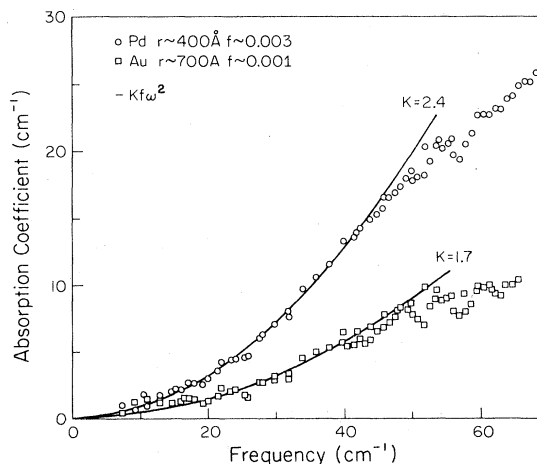


FIG. 6. Far-infrared absorption coefficient of Pd and Au small particles. A fit to a quadratic curve is also shown.

particles, the absorption coefficient of the Al particles increases rapidly with volume fraction. In Fig. 12 we have plotted on logarithmic scales the normalized absorption coefficient versus concentration. These data were calculated by dividing the absorption coefficient for the 0.003 and 0.03 samples by the absorption coefficient of the 0.01 sample. Values of this ratio at several different frequencies are plotted in Fig. 10. Data are shown for three different radii, for which the absorption coefficients themselves varied by an order of magnitude. The increase in this normalized absorption coefficient is clearly more rapid than linear, although not quite as strong as the  $f^2$  curve shown on the plot. The deviation from a linear dependence implies strongly that the far-infrared absorption in these samples does not arise from simple single-particle effects.

The results of our measurements on Al composites are summarized in Table II, which gives the median particle radius, volume fraction, experimental values for the coefficient of the quadratic absorption coefficient for our samples and for the Al powder samples of Granqvist *et al.*<sup>2</sup>

TABLE I. Ag, Au, Pd, and PdH<sub>0.8</sub> composite systems.

Material	Particle radius (Å)	Volume fraction	$K_{\text{expt}}$ (cm)	$K_{\text{theor}}$ (cm)	Notes
Ag	400	0.003	1.4	0.024	in KCl
Ag	400	0.01	1.1	0.024	
Au	700	0.002	1.7	0.15	in Al <sub>2</sub> O <sub>3</sub> powder
Pd	200	0.003	1.9	0.0012	in Al <sub>2</sub> O <sub>3</sub> powder
Pd	400	0.003	2.4	0.010	in Al <sub>2</sub> O <sub>3</sub> powder
PdH <sub>0.8</sub> <sup>a</sup>	400	0.003	2.4	0.008	

<sup>a</sup>Converted from Pd by exposure to hydrogen.

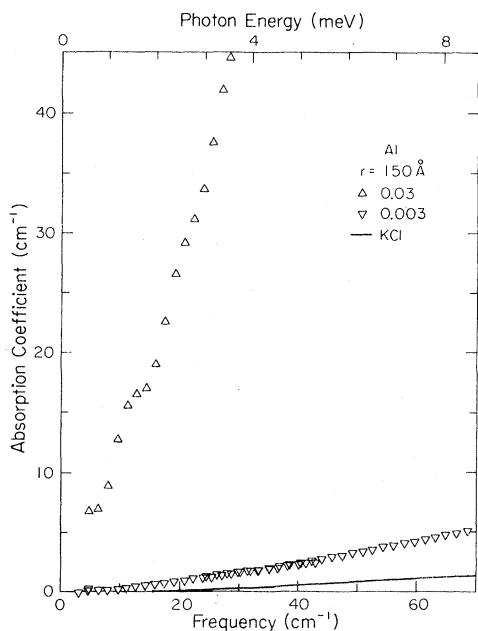


FIG. 7. Far-infrared absorption coefficient of 150-Å radius Al particles in KCl. Data are shown for metal volume fractions of 0.003 and 0.03.

and Tanner *et al.*<sup>1</sup> Theoretical values of the absorption coefficient are also included.

Note that two experimental values of  $K$  are shown in Table II, the first based on the volume fraction of metal obtained from the weights of two con-

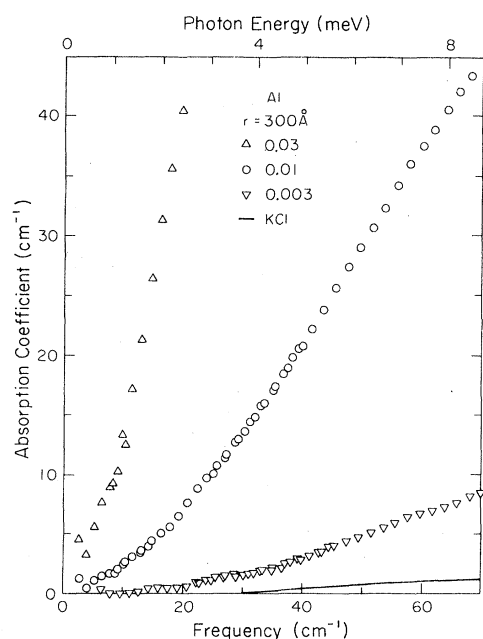


FIG. 8. Far-infrared absorption coefficient of 300-Å radius Al particles in KCl. Data are shown for metal volume fractions of 0.003, 0.01, and 0.03.

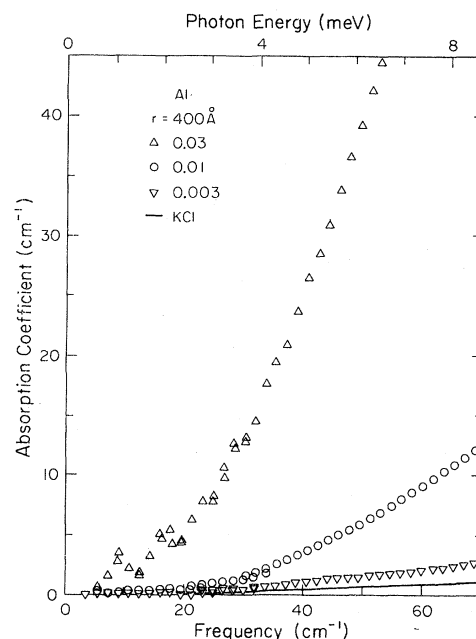


FIG. 9. Far-infrared absorption coefficient of 400-Å radius Al particles in KCl. Data are shown for metal volume fractions of 0.003, 0.01, and 0.03.

stituents of the composites. This uncorrected volume fraction is based on the assumption that the metal particles have no oxide coating. In the second case we have reduced the metal volume fraction to correct for the possible presence of an oxide coating, assumed to have thickness  $t$  of about 10 Å.<sup>14</sup> Although the particle has radius  $a$ , the radius of metal is only  $a - t$ ; the volume fraction of metal is therefore reduced, leading to a corrected coefficient,

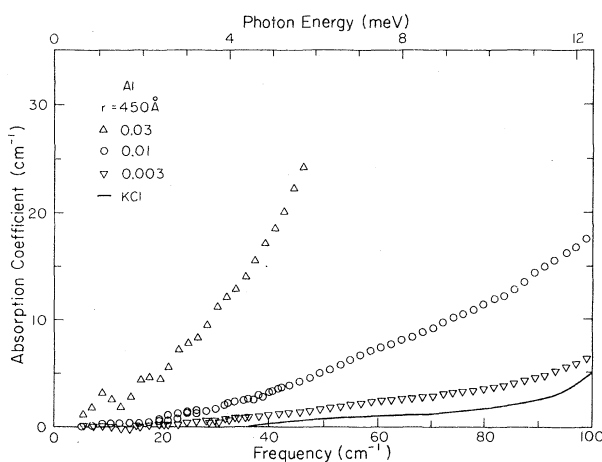


FIG. 10. Far-infrared absorption coefficient of 450-Å radius Al particles in KCl. Data are shown for metal volume fractions of 0.003, 0.01, and 0.03.

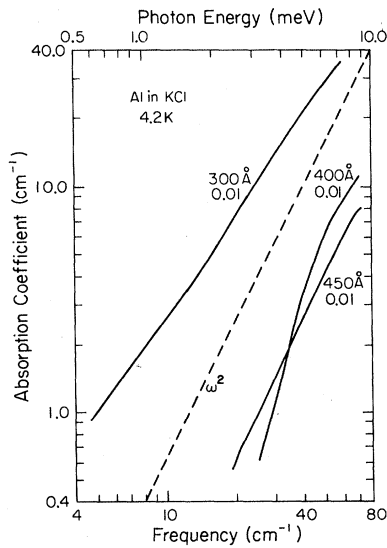


FIG. 11. Far-infrared absorption coefficient of Al small particles in KCl at a volume fraction of 0.01. Data are shown on a log-log scale for particle radii of 300, 400, and 450 Å.

$$K' = K \left( \frac{a}{a-t} \right)^3 \tag{13}$$

This oxide correction is obviously most important for the smaller particles. For the samples of Granqvist *et al.*,<sup>2</sup> the volume fraction of metal is reduced by about a factor of 4.

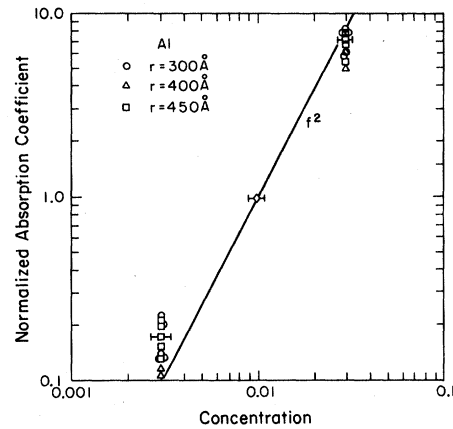


FIG. 12. Normalized absorption coefficient for Al particles in KCl versus metal volume fraction. The data for volume fractions of 0.003 and 0.03 have been normalized by dividing by the absorption coefficient of the 0.01 volume fraction sample.

In allowing for the presence of an oxide coating, there is an implicit assumption that the oxide is not absorbing. Figure 13 shows the measured absorption coefficient of Al<sub>2</sub>O<sub>3</sub> powder dispersed in KCl. The Al<sub>2</sub>O<sub>3</sub> powders were Linde<sup>15</sup> polishing powder with particle radii of 250 Å ( $\gamma$ -alumina) and 1500 Å ( $\alpha$ -alumina). The absorption coefficient of the  $\alpha$ -alumina, which is crystalline Al<sub>2</sub>O<sub>3</sub>, is not distinguishable from that of the KCl. The absorption coefficient of the  $\gamma$ -alumina, which

TABLE II. Aluminum- $\alpha$ -aluminum oxide composite systems.

Material	Particle radius (Å)	Volume fraction	$K_{\text{expt}}$ (cm)	$K'_{\text{expt}}$ <sup>a</sup>	$K_{\text{theor}}$ (cm)	Notes
Al	25	0.015	0.06	0.28	$3 \times 10^{-5}$	Unsupported <sup>b</sup>
Al	75	0.04	0.08	0.12	$1 \times 10^{-4}$	Unsupported <sup>c</sup>
Al	150	0.003	0.3	0.36	$1.3 \times 10^{-3}$	in KCl
Al	150	0.03	2.0	2.4	$1.3 \times 10^{-3}$	
Al	190	0.04	0.16	0.19	$2.9 \times 10^{-3}$	Unsupported <sup>c</sup>
Al	200	0.04	0.21	0.24	$3.0 \times 10^{-3}$	Unsupported <sup>c</sup>
Al	300	0.003	0.52	0.58	0.010	in KCl
Al	300	0.01	1.6	1.8	0.010	
Al	300	0.03	4.0	4.4	0.010	
Al	400	0.003	0.12	0.13	0.024	in KCl
Al	400	0.01	0.21	0.23	0.024	
Al	400	0.03	0.50	0.54	0.024	
Al	450	0.003	0.16	0.17	0.035	in KCl
Al	450	0.01	0.18	0.19	0.035	
Al	450	0.03	0.39	0.42	0.035	
Al <sub>2</sub> O <sub>3</sub> <sup>d</sup>	250	0.01	0.013			in KCl
Al <sub>2</sub> O <sub>3</sub>	250	0.05	0.015			
Al <sub>2</sub> O <sub>3</sub>	250	0.15	0.005			Unsupported

<sup>a</sup>Assumes a nonabsorbing oxide layer 10 Å thick.

<sup>b</sup>Data of Granqvist *et al.*, Ref. 2.

<sup>c</sup>Data of Tanner *et al.*, Ref. 1.

<sup>d</sup> $\gamma$ -alumina.

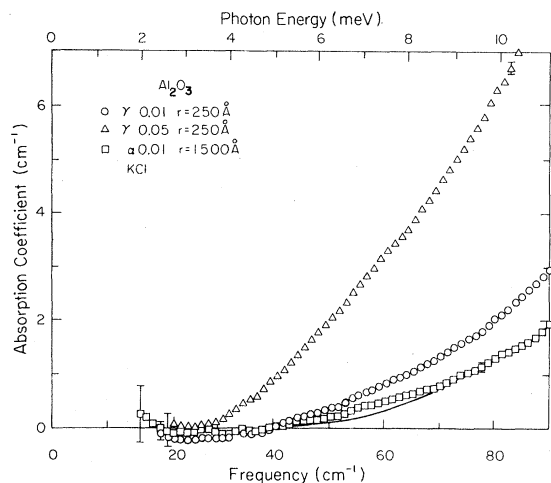


FIG. 13. Far-infrared absorption coefficient of  $\text{Al}_2\text{O}_3$  particles in KCl. Data are shown for two-particle radii (250 and 1500 Å).

contains a large number of defects, is larger than that of the  $\alpha$ -alumina but nowhere near as large as that of the metal particles.

#### V. DISCUSSION

The far-infrared absorption in small metallic particles is larger than the prediction of the MGT and EMA, discussed in Sec. II. Although the absorption coefficient is quadratic in frequency in the far infrared, this frequency dependence cannot continue forever. The frequency at which the quadratic frequency dependence stops may be estimated using the oscillator strength sum rule

$$\int_0^{\infty} \sigma_1(\omega) d\omega = \frac{\pi n_e e^2}{2m}. \quad (14)$$

In Eq. (14),  $\sigma_1(\omega)$  is the frequency-dependent conductivity of the material,  $n_e$  the electronic density,  $e$  the electronic charge, and  $m$  the electronic mass. For the small particle samples we can write

$$\sigma_1(\omega) = \frac{cn}{4\pi} \alpha(\omega), \quad (15)$$

where  $n$  is the refractive index of the material. In addition, the electron density in the composite sample is related to the plasma frequency of the metallic constituent  $\omega_p$  by

$$\frac{4\pi n_e e^2}{m} = f \omega_p^2, \quad (16)$$

where  $f$  is the volume fraction of metal.

The substitution of Eqs. (15) and (16) into (14) gives a sum rule for  $n\alpha$

$$\int_0^{\infty} n\alpha(\omega) d\omega = \frac{\pi}{2c} f \omega_p^2. \quad (17)$$

We now assume a model for the absorption coefficient of the form

$$\alpha = \begin{cases} Kf\omega^2, & \omega \leq \omega_0 \\ Kf\omega_0^2, & \omega_0 \leq \omega \leq \omega_p \\ 0, & \omega > \omega_p. \end{cases} \quad (18)$$

According to this model the absorption coefficient is quadratic below a frequency  $\omega_0$ , constant between  $\omega_0$  and the plasma frequency  $\omega_p$ , and zero (i.e., transparent) above  $\omega_p$ . The frequency that we are trying to estimate is the crossover frequency  $\omega_0$ . The refractive index is assumed constant, equal to that of the host material  $n=2.2$ .

Substituting these quantities into Eq. (17), the frequency  $\omega_0$  is found to be

$$\omega_0^2 = \frac{\pi}{2cnK} \omega_p^2, \quad (19)$$

where we have neglected a second, smaller term. Using  $K=2$  cm and  $\omega_p=5 \times 10^4$   $\text{cm}^{-1}$ , we obtain  $\omega_0=300$   $\text{cm}^{-1}$ .

This sum-rule argument implies that no matter what the origin of the far-infrared absorption, it cannot continue at frequencies above about 300 to 1000  $\text{cm}^{-1}$  (depending upon parameters used) but must instead level off. This tendency to saturate is seen in the far-infrared absorption of large particles, both in the theoretical plots of Fig. 2 and in the experimental data<sup>4</sup> on Pd particles with  $a \sim 1$   $\mu\text{m}$ .

One reason for our interest in small metal particles is the possibility of observing effects arising from size quantization of the electron energy levels in the particles. This effect, as proposed by Gor'kov and Eliashberg,<sup>18</sup> would modify the dielectric function of the metal particle and, perhaps, introduce structure into the absorption coefficient of the composite materials at frequencies near the mean energy-level spacing in the particles  $\Delta \sim E_F/N$ , where  $N$  is the total number of conduction electrons in the particle and  $E_F$  the Fermi energy. Devaty and Sievers<sup>19</sup> have recently described corrections to this theory. They conclude that the predicted structure is unobservable in practice because of the size distribution of the particles. In addition, the absorption coefficient predicted by the quantum theory is smaller than found experimentally by about 3 orders of magnitude.<sup>2,11,19</sup>

For quantum-mechanical effects to be important, the particle must be at a temperature low enough that thermal energies do not smear the Fermi surface over many energy levels. This tempera-

ture is  $T \sim \Delta \sim E_F/n\Omega$ , where  $n$  is the conduction electron density and  $\Omega$  is the particle volume. With  $E_F \sim 10^4$  K and  $n \sim 10^{23}$ , our smallest particles (with 150 Å radii) would have to be measured at  $\sim 0.01$  K instead of the 4.2 K actually used. The very high temperature at which our measurements were made justifies our neglect of these quantum size effects.

Simanek<sup>5</sup> has attributed the large far-infrared absorption in small metal particles to the oxide coating on the metal surface. In his model the particles were assumed to be aggregated into chains. The small depolarization factor of these chains (for electric field along the chain), as well as the presence of a metallic core to the particles, enhanced the absorption by about a factor of 10 over what it would have been if the particles were all isolated oxide spheres. He then assumed a relatively large value for  $\text{Im}(\epsilon)$  of the oxide and obtained a far-infrared absorption coefficient nearly equal to that observed by Granqvist *et al.*<sup>2</sup>

Our samples are in some cases a factor of 10 more absorbing than those of Ref. 2. (See the third column of Table II.) In addition, our measurements of the absorption of alumina show that both the alpha and the highly defected gamma forms are quite transparent; the  $\text{Al}_2\text{O}_3$  samples were a factor of 10 to 100 less absorbing than our oxide-coated Al composite samples. (See Table II and Fig. 13.) While not completely unambiguous, these results suggest that the anomalous far-infrared absorption does not come from the oxide coating. The ambiguity arises because the oxide on the particle surface might have different optical properties than the alumina. Sievers<sup>20</sup> measured the absorption by totally oxidized Al smoke, in powder form, and found an absorption comparable to that of oxide-coated metal particles; the magnitude was approximately that reported by Granqvist *et al.*<sup>2</sup> As shown in Table II, however, these

powder samples have much less absorption than do our somewhat larger particles. In addition, to obtain high absorption Simanek's mechanism requires that the particles be aggregated into chains.<sup>5,6</sup> Our sample preparation procedure—embedding the particles in a KCl host—should provide a more random distribution than in a powder sample, reduce particle aggregation, and lower the absorption resulting from this mechanism. Our observation of anomalously large absorption implies that the oxide is not the dominant loss mechanism in small-particle composites.

The most interesting result to come from this study is that the far-infrared absorption of the Al composite samples is not linear in the metal volume fraction. Instead, the absorption is almost a quadratic function of the volume fraction. This behavior differs from what occurs in composite samples of Pd in KCl,<sup>3,4</sup> where a very linear behavior was observed for volume fractions between 0.001 and 0.03. It also differs from the behavior of the noble metal smokes described here. A quadratic concentration dependence of absorption might imply that interaction between pairs of particles governs the far-infrared absorption of small-particle-composite systems. This interaction might arise from tunneling through oxide layers separating adjacent particles or from direct electrical contact between particles. However, we do not know why the behavior should occur in Al composite samples and not occur in composites containing other metals.

#### ACKNOWLEDGMENTS

We thank D. Stroud and W. J. Lamb for many interesting discussions on this subject. This research was supported by the U. S. Department of Energy through Contract No. DE-AS02-78ER04914.

<sup>1</sup>D. B. Tanner, A. J. Sievers, and R. A. Buhrman, *Phys. Rev. B* **11**, 1330 (1975).

<sup>2</sup>C. G. Granqvist, R. A. Buhrman, J. Wyns, and A. J. Sievers, *Phys. Rev. Lett.* **37**, 625 (1976).

<sup>3</sup>N. E. Russell, G. L. Carr, and D. B. Tanner, in *Electrical Transport and Optical Properties of Inhomogeneous Media*, edited by J. C. Garland and D. B. Tanner (American Institute of Physics, New York, 1978), p. 263.

<sup>4</sup>N. E. Russell, J. C. Garland, and D. B. Tanner, *Phys. Rev. B* **23**, 632 (1981).

<sup>5</sup>E. Simanek, *Phys. Rev. Lett.* **38**, 1161 (1977).

<sup>6</sup>R. Rupp, *Phys. Rev. B* **19**, 1318 (1979).

<sup>7</sup>A large number of articles and references may be found in *Electrical Transport and Optical Properties*

*of Inhomogeneous Media*, edited by J. C. Garland and D. B. Tanner (American Institute of Physics, New York, 1978).

<sup>8</sup>J. C. Maxwell Garnett, *Philos. Trans. R. Soc. (London)* **203**, 385 (1904); **205**, 237 (1906).

<sup>9</sup>D. A. G. Bruggeman, *Ann. Phys. (Leipzig)* **24**, 636 (1935).

<sup>10</sup>D. Stroud and F. P. Pan, *Phys. Rev. B* **17**, 1602 (1978).

<sup>11</sup>C. G. Granqvist, *Z. Phys. B* **30**, 29 (1978).

<sup>12</sup>D. Stroud, *Phys. Rev. B* **19**, 1783 (1979).

<sup>13</sup>L. D. Landau and E. M. Lifshitz, *Electrodynamics of Continuous Media* (Pergamon, New York, 1960), Secs. 72 and 73.

<sup>14</sup>C. G. Granqvist and R. A. Buhrman, *J. Appl. Phys.* **47**, 2200 (1976).

<sup>15</sup>Linde Corporation, San Diego, CA.

<sup>16</sup>R. L. Henry and D. B. Tanner, *Infrared Phys.* 19, 163 (1979).

<sup>17</sup>H. E. Scott and R. B. Sanderson, *Appl. Opt.* 10, 1097 (1971).

<sup>18</sup>L. P. Gor'kov and G. M. Eliashberg, *Zh. Eksp. Teor. Fiz.* 48, 1407 (1965) [*Sov. Phys.—JETP* 21, 940 (1965)].

<sup>19</sup>R. P. Devaty and A. J. Sievers, *Phys. Rev. B* 22, 2123 (1980).

<sup>20</sup>A. J. Sievers (unpublished).